

CONDENSATION FROM GAS-VAPOR MIXTURES IN SMALL NON-CIRCULAR TUBES

S. Krishnaswamy, H. S. Wang, J. W. Rose

Department of Engineering, Queen Mary, University of London, Mile End Road, London E1 4NS, UK
h.s.wang@qmul.ac.uk; j.w.rose@qmul.ac.uk

ABSTRACT

Careful measurements have been made during condensation of steam inside a small non-circular horizontal tube under forced convection conditions and in the presence of air. The ranges of the relevant variables covered (inlet temperature, pressure, air mole fraction and mixture mass flow rate) were chosen to simulate those occurring in an exhaust heat-exchanger tube of a proposed fuel-cell engine. The experimental tube was cooled by water in laminar counter-flow to simulate the external heat-transfer coefficient (air flowing over fins) in the application. The total heat-transfer rate was found from the mass flow rate and temperature rise of the coolant. The tube wall temperature was measured by thermocouples attached in grooves along its length. Special arrangements were made to ensure good mixing of the coolant (in laminar flow) prior to measuring the inlet and outlet temperatures. The condensate was separated using a cyclone at exit from the tube. A simple model was developed to predict local and total heat-transfer and condensation rates and local bulk vapor composition, temperature and pressure along the tube in terms of the inlet parameters and the wall temperature distribution. The measured heat-transfer and condensation rates for the tube were found to be in good agreement with the calculated values without having recourse to empirical adjustment.

INTRODUCTION

On-board water management is important for fuel-cell powered motor vehicles. The objective of the present investigation was to develop and validate a model for use in design of an exhaust condenser for an automotive fuel-cell engine. For given inlet conditions (temperature, pressure, composition and flow rate) and specified distribution of wall temperature, the model determines the local heat flux, condensation mass flux, temperature, composition and pressure along the tube. The total condensation and heat-transfer rates for a tube of given length are readily calculated. In the application the model would be used with a standard approach for the external air-side (cross flow with fins) and an iterative scheme used to determine the distribution of wall temperature along the tube.

An apparatus has been designed and built in which steam-air (air for convenience) mixtures were passed through a tube cooled externally by water flowing in an annulus in counter flow. Laminar flow of the coolant was required to simulate the exterior heat-transfer resistance in the application. Special coolant mixing arrangements were made to ensure accurate mean temperatures were obtained at inlet and exit of the coolant stream. Surface temperatures at several positions along the tube were measured by embedded thermocouples. The ranges of temperature, pressure, composition and flow rate covered those anticipated in the application.

The measured condensation and heat-transfer rates for the tube agreed with the calculated values to within 20%. No empirical adjustment to the model was needed.

APPARATUS AND PROCEDURE

A flow diagram of the apparatus is shown in Figure 1. Steam was generated in a stainless steel evaporator fitted with two stainless steel sheathed 1 kW electric heaters. Air was injected via a humidity measuring box

and flow meter through a sparge tube at the base of the evaporator. A carry-over suppressor, superheater (500 W) and mixer were located at exit from the evaporator. Temperature and pressure were measured at inlet and exit of the tube. The length and hydraulic diameter of the tube were 1 m and 3 mm respectively. A cyclone separator was located at the tube exit to separate the condensate which was lead to a measuring cylinder while the saturated air was removed via an exit at the top of the separator. The apparatus was well insulated. Cooling water, supplied from a constant head tank,

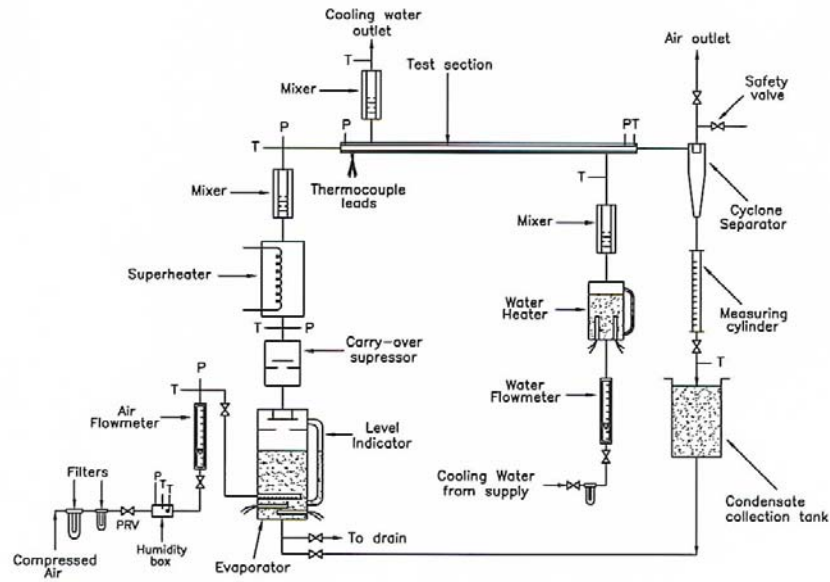


Fig. 1 Flow diagram of test rig

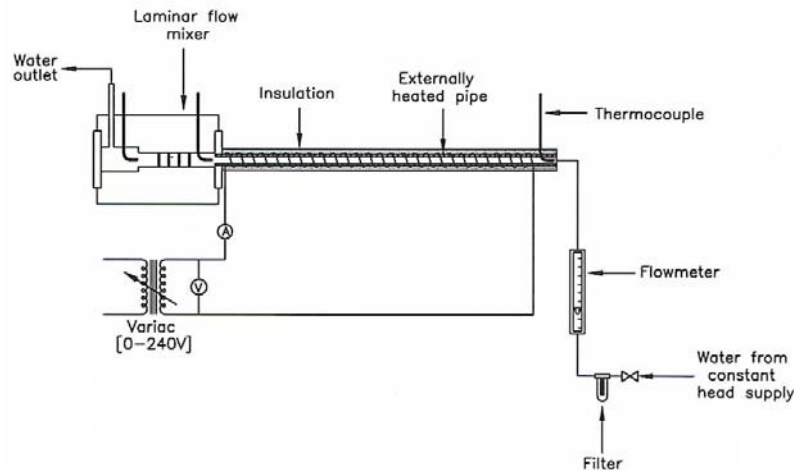


Fig. 2 Test rig for laminar flow mixing box

passed through a flow meter, heater and mixer to the ptfе (Teflon) casing holding the tube so that the coolant flowed in the annular space well insulated externally. As well as the inlet and exit coolant temperatures, the inlet-to-exit temperature difference was measured directly using a 10-junction thermopile. All thermocouples were calibrated against a platinum resistance thermometer in a high precision constant temperature bath. Special attention was paid to adequacy of isothermal immersion of all thermocouple junctions. Full details of the apparatus are given by Krishnaswamy (2004).

The problem of obtaining accurate mixed mean fluid temperatures in laminar flow has been highlighted by Fujii (1992). Mixers, consisting of a ptfе (Teflon) body with an internal copper tube in which were located, at intervals, brass baffles with holes alternately near the centre and perimeter (details of the mixers are given by Krishnaswamy (2004), were manufactured and tested. Figure 2 shows the simple test apparatus in which water was supplied to the mixer from an externally heated tube. Traversing thermocouples measured the temperature distribution across the inlet and exit of the mixer. Specimen results are shown in Figure 3 which clearly indicates both the necessity for mixing arrangements and the satisfactory performance of the design adopted.

All measurements were made under steady conditions. The air mass flow rate was measured directly using the flow meter with appropriate temperature and pressure corrections. The steam mass flow rate was found using an energy balance (steady state power required to evaporate steam plus power required to heat the air in steady flow set equal to the evaporator input power) incorporating a small predetermined heat loss to the surroundings. To assess the reliability of the apparatus and method, tests were first performed using only steam. The heat-transfer rate from the tube, as measured by the coolant flow rate and temperature rise, agreed in all cases with that found from an energy balance for the stream flowing through the tube to within 2.5%. The evaporation rate agreed with the condensate collected to within 1%. Ninety four test runs were then made with steam-air mixtures covering the ranges of inlet pressure, temperature, steam mole fraction, steam-air flow rate and coolant inlet temperature which would be used in the application. A measured wall temperature distribution in a typical run is illustrated in Figure 4. The temperature distributions were fitted by equations of the form:

$$T = A e^{-Bx} + C \quad (1)$$

where A , B and C are constants, for use when making comparisons with the model.

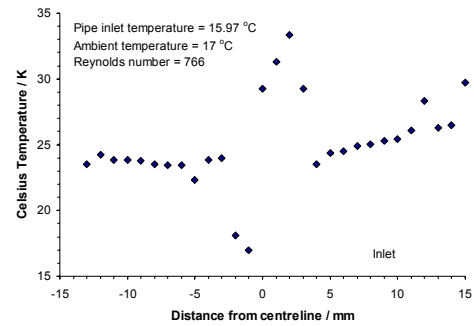


Fig. 3(a) Temperature profile across inlet to mixer

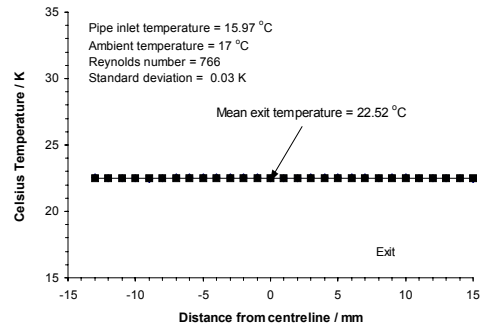


Fig. 3(b) Temperature profile across outlet from mixer

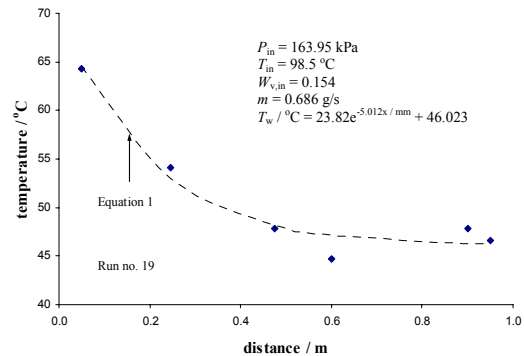


Fig. 4 Measured wall temperature distribution along the condensing tube (Run 19)

MODEL

For the high gas concentrations in the exhaust stream and consequent low condensation mass fluxes, the expected condensation regime is a thin laminar film on the tube wall. For the conditions of the test runs the maximum calculated condensate film thickness (at the

end of the tube for the highest condensation rate case) was 0.07 mm. The flow rate range and channel dimensions indicated that the gas-vapor flow should be turbulent. For the conditions of the test runs the lowest air-steam Reynolds number was around 3400. With these considerations a simple model, applicable to any gas-vapor mixture, has been developed using well-established, heat-mass transfer analogy methods.

The problem is illustrated in Figure 5. The tube is divided into segments of given step length. While the wall temperature is higher than the local bulk saturation temperature, the single-phase, gas-vapour flow is treated using the correlation of Gnielinski (1976):

$$Nu = \frac{a_g d_h}{k} = \frac{(f/2)(Re-1000)Pr}{1+12.7(f/2)^{0.5}(Pr^{2/3}-1)} \quad (2)$$

The friction factor in Eq. (2) and, hence pressure drop, were obtained from the Filonenko (1954) correlation:

$$f = (1.58 \ln Re - 3.28)^{-2} \quad (3)$$

and

$$\tau_i = \frac{1}{2} f \rho u^2 \quad (4)$$

Momentum and energy balances for a segment give the temperature and pressure at the entry to the succeeding segment (and hence the temperature and pressure distribution along the channel) as well as the heat-transfer rate to the wall. When the wall temperature just becomes lower than the equilibrium saturation temperature (dew point) condensation commences. Neglecting gravity, the Nusselt approximations give, for the condensate film

$$\frac{d}{dx} (\tau_i \delta^2) = \frac{2\mu_1 k_1 \Delta T}{\rho_1 h_{fg} \delta} \quad (5)$$

from which the finite difference equation may be rearranged to give

$$\delta_{j+1} = \sqrt{\frac{\left(\frac{2\mu_{1,j} k_{1,j} \Delta T_j \Delta x}{\rho_{1,j} \delta_{j+1} h_{fg,j}} \right) + \tau_{i,j} \delta_j^2}{\tau_{i,j+1}}} \quad (6)$$

The friction factor and surface shear stress were again obtained from Eqs. (3) and (4). Correction to take account of “suction” as described by Kays and Crawford (1993) was incorporated, but had negligible effect for the

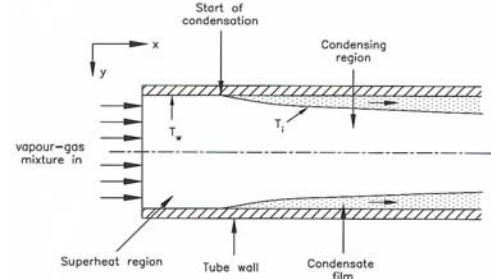


Fig. 5 Schematic view of physical model

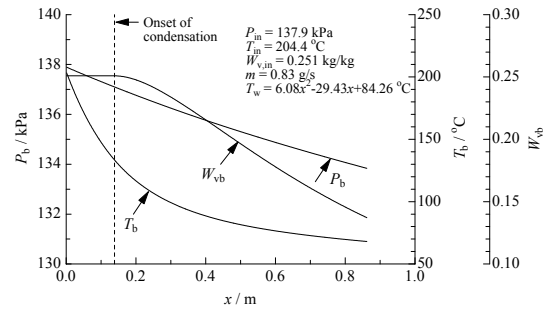


Fig. 6 Model specimen results showing variation of bulk pressure, temperature and vapor mass fraction along the condensing tube

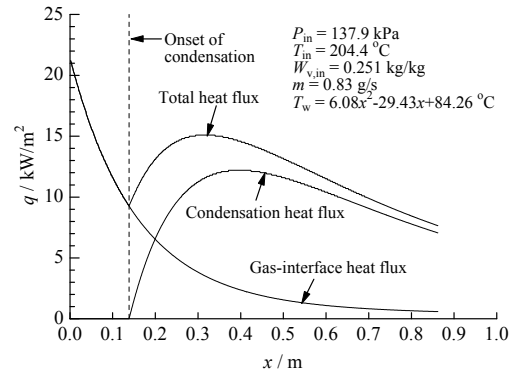


Fig. 7 Model specimen results showing variation of heat flux along the condensing tube

small condensation rates for the conditions investigated. The convective heat transfer from the bulk gas-vapour stream to the condensate surface was found using Eq. (2). Again, correction for “suction” was included but had negligible effect (for details see Krishnaswamy (2004)). For the element under consideration the heat transfer by

convection from the gas and resulting from condensation was equated to the wall heat flux thus:

$$\dot{q}_w = \frac{k_1 \Delta T}{\delta} = \dot{m}_c h_{fg} + \alpha_g (T_b - T_i) \quad (7)$$

The condensation mass flux was obtained from

$$Sh = \left(\frac{\dot{m}_c d_h}{\rho D} \right) \frac{1 - W_{vi}}{(W_{vb} - W_{vi})} \quad (8)$$

which arises from the impermeability condition for the non-condensing gas at the interface. Sh was obtained by analogy (valid for low condensation rates) from equation (2) writing Sh for Nu and Sc for Pr and the mass fraction of gas at the condensate surface is given by the interface equilibrium condition for ideal gas mixtures:

$$W_{ai} = \frac{P_b - P_s(T_i)}{P_b - \left[1 - \left(\frac{M_v}{M_a} \right) \right] P_s(T_i)} \quad (9)$$

Equations (6-9) were solved by a suitable iterative scheme to give the local condensate film thickness, the interface temperature and composition and the condensation mass flux. Momentum, energy and mass balances for the bulk gas-vapour stream gave the pressure, temperature and composition at exit from an element to be used as the entry values for the succeeding element.

The whole process was repeated using smaller step lengths until satisfactory convergence was obtained.

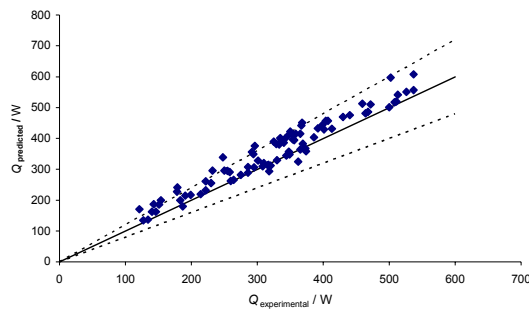


Fig. 8 Comparison of predicted and experimental heat transfer rates

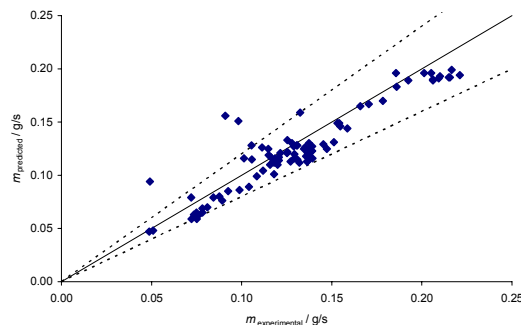


Fig. 9 Comparison of predicted and experimental condensation rates

Properties were taken, for convenience, at the inlet to each segment. Specimen results for parameters specified by the manufacturer (Modine Manufacturing Company) are given in Figures 6 and 7.

COMPARISON WITH MEASUREMENTS AND CONCLUSION

The experimental data are compared with the model calculations in Figures 8 and 9. It is seen that the model predicts both heat transfer and condensation rate generally within about 20% tending generally to over predict the heat transfer. However, these results were considered satisfactory for design purposes and no empirical adjustment of the model was considered necessary.

NOMENCLATURE

A	constant in wall temperature distribution, see Eq. (1)
B	constant in wall temperature distribution, see Eq. (1)
C	constant in wall temperature distribution, see Eq. (1)
c_p	specific isobaric heat capacity of vapor-gas mixture
d_h	hydraulic diameter of condensing tube
D	vapor-gas mixture diffusion coefficient
f	friction factor
h_{fg}	specific enthalpy of evaporation
j	segment number
k	thermal conductivity of vapor-gas mixture
k_l	thermal conductivity of condensate
m	mass flow rate of vapor-gas mixture
\dot{m}_c	local condensation mass flux
M_a	molar mass of non-condensing gas, i.e. air
M_v	molar mass of vapor, i.e. steam
Nu	Nusselt number
P_s	saturation pressure
Pr	Prandtl number of vapor-gas mixture
\dot{q}_w	heat flux to tube wall
Sc	Schmidt number of vapor-gas mixture
Sh	Sherwood number of vapor-gas mixture
T	thermodynamic temperature
T_i	interface temperature
T_b	bulk temperature of vapor-gas mixture
u	bulk vapor-gas mixture velocity
W_{ai}	mass fraction of non-condensing gas, i.e. air at the liquid-gas interface
W_v	mass fraction of vapor
W_{vi}	mass fraction of vapor at the liquid-gas interface

W_{vb}	bulk stream mass fraction of vapor
ΔT	temperature difference across condensate film
Δx	segment length
α_g	convective surface heat-transfer coefficient for vapor-gas mixture
δ	condensate film thickness
μ	viscosity of vapor-gas mixture
μ_1	viscosity of condensate
ρ	density of vapor-gas mixture
ρ_1	density of condensate
τ_i	shear stress on condensate film

subscripts

a	air
b	bulk
c	condensing
i	interface
j	at entry to segment j
l	condensate
s	saturation
v	vapor
w	wall

ACKNOWLEDGMENTS

The authors gratefully acknowledge financial support from the Modine Manufacturing Company Racine, WI, USA.

REFERENCES

- Fujii, T., 1992, Overlooked factors and unsolved problems in experimental research on condensation heat transfer. *Experimental Thermal and Fluid Science*, Vol.5, pp.652-663.
- Gnielinski, V., 1976, New equations for heat and mass transfer in turbulent pipe and channel flow. *Int. Chem. Eng.*, Vol. 16, pp.359-368.
- Kays, M. W. and Crawford, M. E., 1993, Convective heat and Mass Transfer, 3rd ed. McGraw Hill.
- Krishnaswamy, S., 2004, Filmwise condensation inside a non-circular horizontal tube in the presence of forced convection and a non-condensing gas. PhD Thesis, University of London, UK
- Filonenko, G. K., 1954, Hydraulic Resistance in Pipes. *Teploergetica*, Vol. 1, pp.40-44 (in Russian).